HHS Public Access

Author manuscript

Nat Neurosci. Author manuscript; available in PMC 2014 January 11.

Published in final edited form as:

Nat Neurosci. ; 15(1): 90–97. doi:10.1038/nn.2969.

Inactivity–Induced Increase in nAChRs Up–Regulates Shal K^+ Channels to Stabilize Synaptic Potentials

Yong Ping[1] and **Susan Tsunoda**[1,*]

[1]Department of Biomedical Sciences, Colorado State University, Fort Collins, CO 80528 USA

Abstract

Long–term synaptic changes, which are essential for learning and memory, are dependent on homeostatic mechanisms that stabilize neural activity. Homeostatic responses have also been implicated in pathological conditions, including nicotine addiction. Although multiple homeostatic pathways have been described, little is known about how compensatory responses are tuned to prevent them from overshooting their optimal range of activity. We show that prolonged inhibition of nicotinic acetylcholine receptors (nAChRs), the major excitatory receptor in the *Drosophila* CNS, results in a homeostatic increase in the Dα7 nAChR. This response then induces an increase in the transient A–type K^+ current carried by Shal/K_v4 channels. While increasing Dα7 boosts mEPSCs, the ensuing increase in Shal channels serves to stabilize postsynaptic potentials. This identifies a novel mechanism to fine–tune the homeostatic response.

Introduction

Maintaining neural activity within an optimal range, while at the same time, allowing for the storage of long–term changes in synaptic strength is an important challenge of the nervous system[1]. Homeostatic synaptic plasticity has widely been received as a mechanism by which neuronal circuits preserve stability when presented with changes in activity. Synaptic inactivity has been shown to result in an increase in postsynaptic GluA1/GluA2 receptor number and/or presynaptic vesicle release in mammalian neurons, as well as at the neuromuscular junction (NMJ)[1–3]. Although multiple homeostatic feedback mechanisms exist for scaling up synaptic strength, maintaining activity within an optimal range must also require precise tuning of activity to prevent over–shooting the target range. Downstream control mechanisms are likely to exist, although no examples have been reported.

Most cell intrinsic responses to activity blockade have been reported to contribute to the homeostatic response[4–6]. For example, in cultured cortical pyramidal neurons, activity blockade results in an increased voltage–dependent Na^+ current and a reduced delayed rectifier type K^+ current, both predicted to increase excitability[4]. In contrast, however,

*Corresponding Author, phone: 970–491–3665, FAX: 970–491–7907, susan.tsunoda@colostate.edu.

Author Contributions

Y.P. conducted all of the experiments and analyzed all of the data. S.T. supervised the project, and did the majority of writing the manuscript.

deprivation of visual input during the critical period of development reduced intrinsic excitability of pyramidal neurons in the visual cortex[7]. In all cases, little is known about the signaling pathways inducing these intrinsic changes, how these changes are regulated, and their roles in synaptic homeostasis[1].

Homeostasis has also been implicated to underlie the up–regulation of neuronal nicotinic acetylcholine receptors (nAChRs) following prolonged exposure to nicotine[8]. Although nicotine is an agonist, extended exposure to low levels of nicotine leads to desensitization of nAChRs, which is thought to trigger homeostatic pathways[9,10]. The increased number of nAChRs is thought to contribute to the increased sensitivity to nicotine when receptors are available for activation, and conversely, tolerance to nicotine when receptors are desensitized[8,9]. A greater understanding of the homeostatic regulation of nAChRs is likely to provide insight into the pathogenesis of nicotine addiction.

Here, we block nAChRs, which mediate the vast majority of fast excitatory synaptic transmission in central *Drosophila* neurons, and reveal a homeostatic increase in mEPSC carried by newly translated Dα7 nAChRs. We show that this increase in Dα7 induces an increase in expression and function of the transient A–type Shal K^+ channel, and this increase is triggered by increased Ca^{2+} influx through Dα7 receptors and CaMKII activation. While increasing Dα7 boosts mEPSCs, the ensuing increase in Shal K^+ channels evokes a novel mechanism to stabilize synaptic potentials.

Results

Homeostatic Increase in mEPSCs in Excitatory Neurons

To examine homeostatic changes at inter–neuronal synapses in *Drosophila*, we began by using primary cultures from late–gastrula stage embryos. These cultures have been well studied, with respect to voltage–dependent currents and synaptic physiology[11–14], allow the labeling of identified neurons for analysis[15,16], and have been shown to exhibit stable, matured, electrical properties after three days[13]. Since nAChRs mediate the vast majority of fast excitatory synaptic events in the *Drosophila* central nervous system[13,16], we blocked synaptic activity with curare, which completely eliminates mEPSCs (**Supplementary Fig. 1a**). To analyze identified neurons, these specific *GAL4* lines were used to drive expression of *UAS–mCD8–EGFP*: (1) *RRa–GAL4* or *RN2–GAL4* were used to drive expression in aCC and RP2 motoneurons (MNs), (2) *GH146–GAL4* was used to drive expression in projection neurons (PNs), which receive input from olfactory neurons and project to higher centers in the brain, (3) *EL–GAL4* was used to drive expression in the lateral cluster of *even–skipped* expressing cells (EL), which are reported to be exclusively interneurons[17].

We blocked synaptic activity with curare in the culture medium, then washed out antagonist for ~3 minutes, and allowed the cultures to recover for 30 minutes in fresh medium. Medium was then changed to extracellular recording solution and mEPSCs were recorded from EGFP–labeled neurons. This treatment protocol is referred to as Protocol #1 (see Methods). When synaptic activity was blocked for up to 12 hours, no changes in mEPSCs were observed (**Supplementary Fig. 1c–1f**). With 24 hours of synaptic inhibition, however, there was a clear increase in mEPSC amplitude and frequency in the excitatory MNs (Ctr: 11.3 ±

1.1 pA, T: 18.5 ± 2.0 pA) and PNs (Ctr: 8.0 ± 0.9 pA, T: 15.1 ± 1.2 pA) (**Fig. 1a, 1c, 1d, and Supplementary Fig. 1g**). In contrast, EL interneurons showed a slight decrease in frequency, and only immediately after washout of antagonist (**Fig. 1b, 1e, 1f, and Supplementary Fig. 1h**). Enhancement of mEPSCs in excitatory neurons, however, was long–lasting, persisting for hours after antagonist washout (**Fig. 1c, 1d**). Since no significant difference in dendritic branching, quantified at radial intervals from the soma of single neurons, were observed between treated and untreated controls (**Supplementary Fig. 1i**), changes in mEPSCs are not likely to be due to major structural changes induced by curare treatment. Increases in mEPSC amplitude and frequency in MNs and PNs in response to activity blockade are similar to homeostatic responses reported for glutamatergic mammalian neurons. Thus, although mediated by different receptors, excitatory synaptic homeostasis appears to be a conserved phenomenon in central *Drosophila* neurons.

Inactivity-Induced Up–Regulation of the Dα7 nAChRs

An increase in mEPSC amplitude suggests an enhancement in postsynaptic nAChR receptor function and/or number. Interestingly, mEPSCs recorded from curare treated MNs also appeared to displayed a faster rate of decay, compared to untreated MNs (**Fig. 1g**). When mEPSC decays were fit with a double exponential function, we found a similar fast component present in both mock and curare treated MNs (Control τ(fast) = 0.32 ± 0.03 ms, Treated τ(fast) = 0.27 ± 0.03 ms). The contribution of this fast component, however, was significantly increased with synaptic blockade (**Fig. 1g**; $A_1/(A_1+A_2)$). This result suggested that the increased mEPSC amplitudes might be due to up–regulation of a particular subtype of nAChRs. Interestingly, vertebrate α7 nAChRs have been shown to display more rapid deactivation kinetics than other subtypes[18,19]. Although there is a paucity of specific inhibitors, memantine has previously been used to block mammalian α7 receptors[20]. Indeed, we found that the increase in mEPSC amplitude, following curare treatment, was blocked when memantine was used during recording (Ctr: 8.3 ± 0.9 pA, T: 8.7 ± 0.9 pA; **Fig. 1h**), suggesting that the increase is memantine– sensitive, and likely carried by the *Drosophila* α7 (Dα7) receptors. To examine whether the increase in mEPSC amplitude might be due to an increase in Dα7 receptor number, we used an antibody against Dα7 to immunostain cultures that were either mock or curare treated for 24 hours. Indeed, we observed a clear and reproducible increase in Dα7 signal in most neurons, including GFP–labeled MNs, from curare treated cultures (**Fig. 1i**).

We next examined if the increase in Dα7, induced by synaptic blockade, can be observed in adult brains *in vivo*, and further, if this homeostatic response is specific to the Dα7 subunit. To do this, whole brains were mock or curare treated in culture; cell viability was confirmed by showing that protein synthesis could indeed be induced in cultured brains (**Supplementary Fig. 1j**). We incubated wild–type brains in culture medium either with, or without, curare for 15 minutes, 12 hours, or 24 hours; protein levels were analyzed by immunoblot analysis. Strikingly, we found that Dα7 protein levels were increased by more than 60% after 24 hours of curare treatment (**Fig. 1j**), while no differences were observed with shorter incubations. In addition, similar to the enhancement in mEPSCs, the increase in Dα7 protein persisted for at least 5 hours (**Supplementary Fig. 1b**). In contrast, other nAChR subunits, including Dα1, Dα2, Dβ1, and Dβ2 showed no significant change

following synaptic inactivity (**Fig. 1j**). Altogether, our results show a selective increase in Dα7 receptors that likely underlies the increased amplitudes of mEPSCs following prolonged synaptic block.

Inactivity-Induced Increase in Shal K^+ Currents

Homeostasis can be achieved by synaptic and/or cell intrinsic changes. Indeed, other systems have demonstrated cell intrinsic changes after activity blockade[4–7,21]. How these intrinsic changes are triggered in by synaptic inactivity, however, has remained a mystery. We set out to investigate whether cell intrinsic changes also occur in our system, and planned to examine how they are triggered by synaptic blockade. Since all of the voltage–dependent K^+ channels and currents have been genetically and electrophysiologically identified in these cultured neurons[11,12], we first examined whether I_A currents carried by Shal/K_V4 channels, or delayed rectifier (DR) currents carried by Shab/K_V2 and Shaw/K_V3 channels, were changed in response to curare treatment. We blocked synaptic activity with curare for 24 hours using the same treatment Protocol #1 used for mEPSC recordings (see Methods), and performed voltage paradigms to isolate DR and I_A currents. We found that I_A currents carried by Shal K^+ channels were dramatically increased in MNs (from 176 ± 22 to 438 ± 30 pA) and PNs (from 269 ± 26 to 413 ± 35 pA) (**Fig. 2a, 2b**), with no change in cell size, as indicated by capacitance measurements (**Supplementary Table 1**). No changes in I_A and DR currents were observed in EL interneurons (**Supplementary Fig. 3d**). Interestingly, however, if antagonist was not washed out (Protocol #2, see Methods), no changes in I_A or DR currents were observed in either MNs or PNs (**Fig. 2a, 2b**). These results suggest that prolonged synaptic inhibition results in a selective increase in Shal K^+ current density in excitatory neurons. Up–regulation of Shal required recovery of synaptic transmission, but was independent of AP firing, as it occurred even in the presence of TTX (**Fig. 2a, 2b**).

To test whether the increase in I_A is due to an increase in the number of Shal K^+ channels, we examined whole brains following curare treatment. Levels of Shal protein from brains examined right after mock or curare treatment (Protocol #2) were not significantly different (**Fig. 2c**, No wash). If, however, synaptic transmission was allowed to recover for 60 minutes (Protocol #1), there was ~80% increase in Shal protein (**Fig. 2c**, Recovery). Like Dα7, this increase was seen only after 24 hours of curare treatment, and persisted for at least 5 hours (**Supplementary Fig. 3a**). Altogether, our results show that prolonged blockade of synaptic activity results in an increase in Shal K^+ channels that requires recovery of synaptic activity. In contrast, treatment Protocols #1 and #2 both resulted in an up–regulation of Dα7, suggesting that the increase in Dα7 does not require a period of recovery following synaptic blockade (**Fig. 2c**).

Since Shal K^+ currents play an important role in neuronal firing[15], we speculated that the up–regulation of Shal channels should also affect the firing behavior of cells. We curare treated wild–type cultures for 24 hours, washed out antagonist with medium, and then monitored firing during the following 30 minutes (treatment Protocol #3, see Methods), when Shal channels should be actively up–regulated. We compared MN firing patterns, in response to a 500 ms current injection of 60 pA, at 5–10 minutes and then at 25–30 minutes.

We found that the number of APs fired decreased during this recovery period (**Supplementary Fig. 8**). Since Shal channels have been shown to affect both latency to AP firing and firing frequency in these neurons[15,22], these changes are consistent with an increase in Shal channels during this recovery period following synaptic blockade.

To gain insight into whether Shal channels were preferentially up–regulated in a particular subcellular region of neurons, we recorded Shal channel activity in cell–attached patches from the somas and dendrites of MNs. We compared Shal currents in patches from cells that were mock or curare treated; antagonist was washed out and synaptic transmission was allowed to recover for 30 minutes to induce the up–regulation of Shal (Protocol #1, see Methods). Cell–attached patches from dendrites were obtained from a branch point ~30 μm from the soma (**Fig. 2d**). We found that Shal currents were increased with curare treatment in patches from both the cell body and dendrites (**Fig. 2e**). Up–regulation of Shal currents, however, was 1.5–fold larger in dendrites than in the cell body (**Fig. 2e**).

New Synthesis of Dα7 and Shal are Differentially Regulated

The increase in total Dα7 and Shal protein levels, following prolonged synaptic blockade (**Fig. 1, 2**), suggests the involvement of new protein synthesis. To directly test this, and to examine whether regulation occurs at the transcriptional or translational level, we used Actinomycin D (Actino) to inhibit gene transcription, and either Anisomycin (Aniso) or cycloheximide (CXM) to block protein translation. Cultured brains were incubated with Actino (50 μM), CXM (100 μM), or Aniso (40 μM) throughout mock and curare treatment Protocol #1 (**Fig. 3a, 3b**). As expected, the increase in Dα7 and Shal proteins following curare treatment were both blocked by Aniso and CXM (**Fig. 3b, Supplementary Fig. 4a**), confirming that new protein synthesis is required in both cases. Actino, however, only blocked the increase in Shal K^+ channels, but not Dα7 receptors (**Fig. 3a**), suggesting transcriptional regulation of *Shal*.

To further test the differential regulation of Dα7 and Shal K^+, we examined mEPSCs and I_A currents in identified MNs when either transcription or translation was inhibited. We used Actino (50 μM) to block transcription, and Aniso (40 μM) to block protein translation. Synaptic blockade induced an increase in mEPSC and I_A amplitudes, as expected (**Fig. 3c, 3d**). When cultures were incubated with Aniso, the increase in both mEPSC and I_A amplitudes were blocked (**Fig. 3c, 3d**), confirming again the involvement of new protein synthesis. Inhibition of transcription by Actino, in contrast, only blocked the up–regulation of Shal K^+ currents, and not mEPSC amplitudes (**Fig. 3c, 3d**). Thus, immunoblot analyses and electrophysiological recordings both show that synaptic inactivity induces an increase in translation of Dα7 receptors, and an increase in transcription of the *Shal* gene.

Given that the increase in Shal channels occurs, not during the 24 hours of synaptic inhibition, but during the shorter 30–minute period of recovery of synaptic transmission (see above; **Fig. 2**), we were surprised that regulation occurred at the transcriptional level. We further tested this finding by comparing *Shal* expression from the endogenous *Shal* gene, to that from an epitope (HA)–tagged *Shal* transgene (*UAS–HA–Shal*) lacking transcriptional regulatory domains. We generated a transgenic line in which *UAS–HA–Shal* expression is

driven by *RRa–GAL4*. After 24 hours of either mock or curare treatment (Protocol #1), cultures were immunostained using an antibody against either HA or Shal. We found that synaptic blockade did not induce an increase in anti–HA signal, but did induce a clear increase in anti–Shal signal in both soma and dendrites (**Fig. 3e, Supplementary Fig. 4b, 4c**). The increase in Shal protein from the endogenous *Shal* gene, but not an exogenous transgene, is consistent with regulation at the transcriptional level.

Increase in Shal is Dependent on Dα7 nAChRs

We next examined the relationship between the increase in Dα7 receptors and the increase in Shal K^+ channels that both follow prolonged synaptic inactivity. The increase in Dα7 receptors occurs first, since it is evident immediately after curare treatment (**Fig. 2c**). In contrast, the increase in Shal channels and current required a subsequent 30–60 minute recovery period of synaptic transmission (**Fig. 2**). These results suggest that the up–regulation of Dα7 is triggered more "directly" by synaptic inactivity, and that up–regulation of Shal channels might occur in response to this increase in Dα7 receptors. To test this possibility, we first examined whether Shal currents are up–regulated in the absence of Dα7. We used *RRa–GAL4* to drive expression of *UAS–mCD8–GFP* in a *Dα7* null mutant background ($D\alpha7^{P\Delta EY6}$), and recorded mEPSCs and Shal K^+ currents from identified MNs before and after curare treatment (Protocol #1, see Methods); note that in this protocol, cultures were given a 30 minute recovery period to allow for Shal channel synthesis. In contrast to wild–type MNs, we found that Shal K^+ currents in MNs lacking Dα7 were not increased following curare treatment (**Fig. 4a**). Interestingly, mEPSCs were increased with synaptic blockade (Ctr: 8.71 ± 0.55 pA, n = 12; T: 10.98 ± 0.72 pA, n = 11; **Fig. 4b**), although to a lesser extent than in wild–type (**Fig. 1c**), suggesting that either that there is some redundancy or compensation by other nAChR subunits that is revealed or developed in the absence of Dα7.

In addition, we compared Shal protein levels from wild–type and *Dα7* mutant brains, similarly mock or curare treated. Immunoblot analyses showed no up–regulation of Shal protein in the absence of Dα7 (**Fig. 4c, 4d**). Since Dα7 subunits are among three nAChR subunits in *Drosophila* (Dα5, Dα6, Dα7) which are ~60% identical to vertebrate α7 nAChR subunits[23], we also examined a null mutant of *Dα6* ($D\alpha6^{DAS2}$). Prolonged inactivity followed by recovery of synaptic transmission, however, still increased Shal protein levels in the absence of Dα6 (**Fig. 4c, 4d**). Altogether, these results indicate that the increase in Shal K^+ channels following synaptic blockade has a specific requirement for Dα7 receptors.

Ca^{2+} is Essential for the Increase in Shal K^+ Channels

If Shal channel expression is up–regulated by an increase in Dα7 receptors, what is the signaling pathway from Dα7 to *Shal* transcription? We have shown that the increase in Dα7, combined with recovery of synaptic transmission, are key events in this pathway. Since α7 receptors have been reported to display greater Ca^{2+} permeability than other nAChRs[18,19], we tested whether Ca^{2+} is an essential secondary messenger in this pathway. To do this, we used the Ca^{2+} chealator BAPTA in our intracellular recording solution. Cultures were mock or curare treated, antagonist was washed out for three minutes, then individual MNs were monitored by whole–cell recording for the next 20–30 minutes, during which time Shal

currents are actively up–regulated (Protocol #3, see Methods). **Figure 5** shows scatter plots representing Shal K^+ current amplitudes at 25–30 minutes versus at 5–10 minutes. Using normal intracellular solution in the pipet, synaptic blockade increased the ratio of (I_A at 25–30 minutes)/(I_A at 5–10 minutes) from 208 ± 17 to 378 ± 24 pA, as expected (**Fig. 5a, 5b, and Supplementary Fig. 5**). To further confirm that Shal K^+ currents were indeed acutely up–regulated, we used Actino or Aniso to block transcription or translation, respectively, and monitored Shal currents following antagonist washout. Indeed, ratios of (I_A at 25–30 minutes)/(I_A at 5–10 minutes) from single cells were no longer increased (**Supplementary Fig. 5c, 5d**), demonstrating that the increase in Shal currents is a result of transcriptionally up–regulated channels. We then monitored Shal currents after curare treatment with BAPTA included in our intracellular solution. We found that curare treatment no longer increased Shal K^+ currents, and (I_A at 25–30 minutes)/(I_A at 5–10 minutes) ratios were close to 1:1 (197 ± 11 pA / 205 ± 13 pA; **Fig. 5c**), as seen for untreated cells (**Fig. 5a**).

Since nAChRs can also induce Ca^{2+} release from intracellular Ca^{2+} stores, we tested the contribution of Ca^{2+} from internal stores in signaling *Shal* expression. We monitored Shal K^+ currents in individual MNs during the ~25–30 minutes of recovery following synaptic blockade. During this time, we used thapsigargin to deplete intracellular Ca^{2+} stores. Inactivity–induced increases in (I_A at 25–30 minutes)/(I_A at 5–10 minutes) ratios, however, were not blocked by thapsigargin (**Fig. 5d**). Together, our results suggest that the rise in intracellular Ca^{2+}, possibly through new Dα7 receptors, and not intracellular stores, is required for signaling the increase in Shal channels.

CaMKII is Essential for Up–Regulation of Shal

Since Ca^{2+}–calmodulin dependent kinases are well known Ca^{2+} targets in a variety of synaptic plasticity and homeostatic pathways, we investigated their potential role in signaling the up–regulation of *Shal*. Cultures were mock and curare treated by Protocol #1 (see Methods). During the 30 minute recovery period of synaptic transmission following antagonist washout, we used Myr–CaMKIINtide and STO–609 to inhibit CaMKII and CaMKK activity, respectively. While synaptic blockade still increased Shal K^+ current amplitudes in the presence of STO–609, the increase in Shal currents was blocked in the presence of Myr–CaMKIINtide (**Fig. 6a**), suggesting that CaMKII is essential for the up–regulation of Shal channels. These results were further confirmed in whole brains. Curare treatment induced an increase in Shal protein in the presence of STO–609, but this increase was completely blocked with Myr–CaMKIINtide (**Fig. 6b, 6c**). Thus, CaMKII is likely to be the target of the Ca^{2+} influx through new Dα7 receptors, and a key component in the signaling pathway triggering up–regulation of Shal channels.

We next tested whether activation of CaMKII was sufficient to up–regulate Shal K^+ currents. To do this, we used the *UAS–CaMKII.T287D* transgene which encodes a constitutively active form of CaMKII ($CaMKII^{T287D}$)[24]. We used *RRa–GAL4* to drive expression of *UAS–mCD8–EGFP* and *UAS–CaMKII.T287D* in MNs. We found that Shal currents were indeed increased, nearly two–fold, in these MNs compared to wild–type MNs (**Supplementary Fig. 6**), suggesting that active CaMKII alone can up–regulate Shal channels.

The Increase in Shal Stabilizes Synaptic Potentials

Why does the homeostatic up–regulation of Dα7 receptors trigger an increase in a hyperpolarizing current? Most reported cell intrinsic changes to synaptic inactivity increase excitability, thereby contributing to the homeostatic response. An increase in Shal K^+ currents, however, would most likely decrease excitability. One possibility is that the increase in Shal K^+ channels serves as a mechanism to regulate the homeostatic response, keeping potentiation "in check" and preventing over–excitation. To investigate this possibility, we examined the effects of the increase in Shal K^+ currents on synaptic potentials (using treatment Protocol #1, see Methods). Strikingly, we found that while amplitudes of mEPSCs were significantly larger following curare treatment (**Fig. 7f**), mEPSPs were stable (Ctr: 1.78 ± 0.12 mV, T: 1.80 ± 0.14 mV; **Fig. 7a, 7e**); this was not due to a difference in resting membrane potential since control and curare treated neurons displayed similar passive membrane properties (**Supplementary Table 1**).

To test this hypothesis more directly, we recorded from MNs expressing a dominant–negative Shal subunit (DNK_V4) that completely blocks Shal K^+ channel function[15]. In the absence of Shal K^+ channel function, mEPSCs are increased after curare treatment (**Fig. 7b, 7f**), similar to wild–type MNs. Thus, homeostatic up–regulation of Dα7 receptors still occurs, independent of Shal K^+ channel function. We next examined mEPSPs from control and curare treated DNK_V4 MNs. Indeed, synaptic potentials were not stabilized as they were in wild–type MNs. mEPSP amplitudies were significantly larger after synaptic inhibition, in the absence of Shal function (Ctr: 2.5 ± 0.21 mV, T: 4.51 ± 0.30 mV; **Fig. 7c, 7e**), indicating that Shal channels are indeed required for stabilizing synaptic potentials. To test whether this function was specific to Shal channels, we performed the same experiments using a *Shab/K_V2* null mutant (*$Shab^3$*). Although loss of *Shab* removes nearly all of the delayed–rectifier K^+ current present in these neurons[11], mEPSPs remained stabilized after curare treatment (**Fig. 7d, 7e**).

Finally, we also monitored mEPSPs in single neurons during the 30 minutes following antagonist washout (Protocol #3, see Methods). mEPSPs from curare treated neurons were increased at 5–10 minutes, presumably due to the increase in Dα7 receptors, then stabilized to control amplitudes after 25–30 minutes after antagonist washout (**Fig. 7g**). To confirm that the acute mEPSP up–regulation at 5–10 minutes, then stabilization at 25–30 minutes was regulated by translation of *Dα7* and transcription of *Shal*, we repeated these experiments, using Actino or Aniso, to block transcription or translation, respectively. When transcription was blocked, mEPSP amplitudes were increased compared to untreated cells, but were not stabilized after 25–30 minutes (**Supplementary Fig. 7a**). When translation was inhibited, the initial increase in mEPSP amplitude (at 5–10 minutes) was unchanged compared to untreated cells, and remained constant during the 30 minutes of monitoring (**Supplementary Fig. 7b**). Altogether, these results suggest that following curare treatment, Dα7 receptors are translationally up–regulated, resulting larger mEPSPs, then Shal is transcriptionally up–regulated, resulting in the stabilization of mEPSPs. When the mEPSPs were monitored in MNs expressing DNK_V4, increased mEPSP amplitudes were no longer stabilized (**Fig. 7g**). Together, our studies show that the increase in Dα7 receptors following

synaptic inactivity triggers an increase in Shal K^+ channels that serves to stabilize synaptic potentials.

Discussion

Synaptic homeostatic mechanisms serve to stabilize neural circuits in response to changes in activity. Studies of synaptic homeostasis in *Drosophila* have largely focused on the NMJ and underlying presynaptic mechanisms[2]. Reports of homeostatic changes at inter–neuronal synapses in *Drosophila* have mostly been limited to structural changes[25–27]. In this study, we show that inhibition of nAChRs resulted in mEPSCs that were increased in amplitude and frequency, indicating both pre and postsynaptic effects. Focusing on postsynaptic changes, we found that the Dα7 receptor was preferentially increased, mediating mEPSCs with larger amplitudes, faster decay rates, and likely increased Ca^{2+} influx. This homeostatic response, however, does not require the Dα7 receptor, since mEPSCs are increased in the *Dα7* null mutant, suggesting that other nAChR(s) are up–regulated in the absence of Dα7. Thus, excitatory neurons exhibit a resilient homeostatic increase in nAChRs to compensate for conditions of inactivity. It is interesting to note the lack of this same plasticity in EL interneurons. Since interneurons are generally thought to be inhibitory (see[28]), this would also contribute to the homeostatic response. Our results parallel the homeostatic increase in GluA1/GluA2 receptors widely observed, and restricted to excitatory mammalian neurons[1,3].

Activity–dependent plasticity of muscular nAChRs has long been studied during development of the vertebrate NMJ[29]. Perhaps more relevant to our findings, however, is the increase in neuronal nAChRs that occurs following prolonged nicotine exposure[18]. Studies have suggested that desensitization of the receptors to nicotine exposure triggers a homeostatic response that up–regulates nAChRs[8]. In our study, direct antagonist exposure results in an increase in the Dα7 nAChR. Dα7 is highly homologous to the vertebrate α7 subunit, sharing ~60% amino acid identity. In the mammalian CNS, homomeric α7 receptors are one of the most abundant and widely expressed classes of nAChRs[19]. Homeostatic up–regulation of α7 has, interestingly, also been speculated to contribute to the progression of Alzheimer's disease[30]. Thus, *Drosophila* central neurons may provide a useful model for studying mechanisms of neuronal nAChR–mediated homeostasis that contribute to pathological conditions, such as nicotine addiction and Alzheimer's disease.

We show that the inactivity–induced increase in Dα7 is followed by an increase in the voltage–dependent Shal K^+ channel. Shal K^+ channels are highly conserved and underlie the somato–dendritic A–type K^+ current in most neurons[31]. Shal currents have been shown to play important roles in regulating dendritic excitability, backpropagating action potentials, and postsynaptic potentials[32–34]. Our data suggests that inactivity induces a translational increase in Dα7 receptors that mediates larger mEPSCs. While the homeostatic increase in mEPSCs is not dependent on Dα7, we show that the up–regulation of Shal channels requires Dα7. Dα7 receptors likely carry a greater influx of Ca^{2+}, which in turn activates CaMKII, leading to rapid (<30 minutes) up–regulation of Shal channels. Since CaMKII has previously been implicated in receptor homeostasis and Shal channel regulation[35–37], the

localization and regulation of CaMKII will likely be critical to its roles in these different pathways.

What is the function of this up–regulation of Shal K^+ channels observed after synaptic blockade and an increase in Dα7 receptors? Previously, cell intrinsic changes have mostly been suggested to increase excitability and contribute to homeostasis[1,4–6,38]. The up–regulation of Shal K^+ current, however, is intriguing because it is likely to counter homeostatic mechanisms. mEPSPs recorded in cell bodies are likely to represent larger mEPSPs in dendrites[39] that would activate local Shal channels, which in turn, would modulate PSPs. EPSPs, both large and small, have been shown to activate Shal K^+ channels in mammalian neurons, similarly reducing EPSPs[34,40]. Indeed, we found that the increase in Shal current stabilized synaptic potentials that would otherwise be increased by homeostatic pathways. Modulation of synaptic currents to match a fixed, or stable, synaptic potential has been proposed to underlie a homeostatic solution to the difference in dendritic arbor sizes, and input resistances, of *Drosophila* PNs[41]. A more generalized function may be that when activity is lowered/blocked, nAChRs are increased to boost activity, then when circuits run the risk of becoming over–active, Shal K^+ channels are up– regulated to temper synaptic potentials. This represents a novel mechanism for fine–tuning the homeostatic response and preventing over–excitation.

The increase in *Shal* channel transcription in response to increased translation of Dα7 brings up many intriguing questions. For example, why is the up– and down–regulation of activity controlled at two different loci? That is, why not up– and down–regulate *Dα7* for needed increases, or decreases in activity? Since up–regulation of Dα7/nAChRs is rather slow (eg. requiring 24 hours of synaptic blockade to up–regulate), one possibility is that it might not be beneficial for the cell to down–regulate the receptors, given that replacement would likely be slow and leave the cell unable to up–regulate activity rapidly if needed. Rapid up–regulation of Shal channels has perhaps evolved to be a better solution. It will also be important to understand if there is any specificity, or coordination with sites of activity/inactivity, to the trafficking and subcellular localization of Shal K^+ channels.

Supplementary Material

Refer to Web version on PubMed Central for supplementary material.

Acknowledgements

We thank G. Waro for genetic crosses and technical assistance. We thank Dr. H. Bellen for the antibody against Dα7 and the *Dα7* mutant line, Dr. S. Sigrist for the *UAS–Dα7–EGFP* fly line, Dr. M. Fujioka for *RRa–GAL4*, *RN–GAL4*, and *EL–GAL4* fly lines, and Drs. E. Gundelfinger and U. Thomas for the *Drosophila* nAChR antibodies. We also thank C. Yeung for genetic mapping and crosses for the transgenic *HA–Shal* line. S.T. is supported by a grant from the National Institutes of Health (R01 GM083335).

Methods

Fly Stocks

We used *w*^{1118} as wild–type in this study. Dr. M. Fujioka provided *RRa–GAL4*, *RN2–GAL4*, and *EL–GAL4* lines[42]. *Dα7*^{PΔEY6} [43] was provided by Dr. H. Bellen, *Dα6*^{DAS2} [44] and *UAS–CaMKII.T287D*[24] were obtained from the Bloomington *Drosophila* stock center, and *Shab*^{3} [45] was provided by Dr. S. Singh. We generated the transgenic line expressing the dominant– negative Shal subunit (*UAS–DNK*$_V$*4*). In brief, the *Shal2* cDNA was modified to encode an HA tag (YPYDVPDYA) fused to the N–terminus and a phenylalanine substituted for tryptophan at amino acid 362; this transgenic line and its function were previously described [15]. For the *UAS–HA–Shal* transgenic line, we modified to *Shal2* cDNA to include two tandem HA tags in an extracellular loop of the channel (after cysteine 221), then subcloned into the *pUAST* transformation vector. This construct was generated by GenScript, Inc. Microinjection of the *pUAST–HA–Shal2* construct into embryos was performed by Rainbow Transgenic Flies, Inc. We screened, mapped, and balanced transgenic lines into stable stocks by standard procedures.

Whole Brain and Neuronal Cultures

For whole brain cultures, we anaesthetized adult flies (<2 days after eclosion), then submerged in ice–cold Schneider's *Drosophila* medium on a clean glass slide. We dissected brains quickly and carefully with retinas left intact; damaged brains were discarded. We placed 5–6 brains in a 50 μL drop of culture medium (18% fetal bovine serum, 100 units/mL penicillin, 100 ug/mL streptomysin in Schneider's *Drosophila* medium) on a glass coverslip. We incubated cultures in a humidified chamber at room temperature, and refreshed the culture medium every 12 hrs.

For embryonic neuronal cultures, we dissociated embryos aged 5–6 hrs (25 °C, stage 9–10) into culture medium, as previously described [11,12]. Note that for curare treated whole brain cultures, we washed for 1 hr following treatment, while embryonic neuronal cultures were washed for 30 min, as indicated in text. In order to monitor Shal currents or mEPSPs during the washout, we washed cultures for 3 min before recording in external solution.

We subjected cultured neurons and brains to three different treatment protocols described here. Protocol #1: We treated cultures with 30 μM tubocurare (curare) in culture medium, then washed antagonist out with fresh medium for ~3 min and incubated cultures in fresh media for a recovery period of 30–60 min (30 min was used for electrophysiological recordings, 60 min was used for cultured brains), followed by recording (in appropriate recording solution) or immunoblot/immunostaining analysis. Protocol #2: We treated cultures with 30 μM curare in culture medium, then replaced medium with recording solution for recording (with antagonist still present), or we made samples for immunoblot analysis. Protocol #3: We treated cultures with 30 μM curare in culture medium, then washed out antagonist with fresh medium for ~3 min, followed by recording (in appropriate recording solution). All curare treatments were for 24 hrs, unless otherwise specified.

Electrophysiology

We performed all recordings in the perforated–patch (400 ug/ml Amphotericin–B in the pipette), conventional whole–cell, or cell–attached configuration, as indicated. We recorded from GFP–labeled neurons from cultures 7 days after dissociation (7d). To chronically suppress neuronal activity, we incubated cultures with 30 μM curare in culture medium at 6d or 7d for indicated times (15 min, 12 hr and 24h). We exchanged culture medium for external solution (in mM): NaCl, 140; KCl, 2; $MgCl_2$, 6; $CaCl_2$, 0.5; HEPES, 5 (pH 7.2). We added TTX (1 μM) and picrotoxin (10 μM) to the external solution when recording mEPSCs/mEPSPs. We used Choline–Cl instead of NaCl when recording Shal currents, with the exception of Shal recordings in **Figure 5**. In **Figure 5**, we added TTX (1 μM) and nifidipine (10 μM) to the external solution to block sodium and Ca^{2+} currents. We filled electrodes with internal solution (in mM): K– Gluconate, 120; KCl, 20; HEPES, 10; EGTA, 1.1; $MgCl_2$, 2; $CaCl_2$, 0.1 (pH 7.2) for mEPSP/mEPSC and firing pattern recordings in **Figure 7, Supplementary Figure 8** and all Shal current recordings. For Shal current recordings in Figure 5, we included BAPTA (10 mM) in the internal solution which was accommodated by decreasing K–Gluconate to 110 mM. In some cases, we used CsCl instead of K–Gluconate/KCl when recording mEPSCs. For cell–attached recordings, we filled pipettes with (in mM): NaCl, 140; $MgCl_2$, 6; $CaCl_2$, 0.5; HEPES, 5; TTX, 0.001; nifedipine (10 μM) (pH 7.2). Some cell–attached patches contained little to no current, most likely because axons can be easily mistaken for dendrites in these neurons; thus, we did not include currents < 5 pA in amplitude. We performed all recordings at room temperature (22–24 °C). Electrodes resistances for all perforated–patch and whole–cell recordings were 3–8 MΩ; gigaohm seals were obtained in all cases. For cell–attached recordings, electrode resistances were 7–9 MΩ, with > 5 GΩ seals; tips were fire–polished and inspected for uniform diameter.

We isolated Shal currents by prepulse protocol, as previously described [15,46]. Briefly, we obtained total whole–cell K^+ currents using a voltage jump to +50 mV, following a 500 ms prepulse of –125 mV. We used a 500 ms prepulse of –45 mV to completely inactivate Shal currents; the delayed rectifier current activated by a jump to +50 mV was then subtracted from the total K^+ current to obtain the Shal current. We recorded mEPSCs at –70 mV. In current–clamp experiments, we clamped the membrane current at 0 pA and leaky cells (resting membrane potentials above –55 mV) were discarded.

Statistical Analyses

For mEPSCs and mEPSPs, we analyzed more than 50 events from each cell using Clampfit (Axon Instruments). We used 2 min recordings from each cell to ensure that each cell was equally represented in our analyses. mEPSC and mEPSP events were detected with detection thresholds of ~2 pA and ~0.4 mV, respectively. We fit mEPSCs deactivation kinetics with a standard double exponential function: $f(t) = A_1e^{-t/\tau(fast)} + A_2e^{-t/\tau(slow)} + C$. $\tau(fast)$ and $\tau(slow)$ are the time constants for the fast and slow components, and A_1 and A_2 are the amplitudes of the each component, respectively. We generated all data from at least 3 independent experiments; shown as means with standard errors of the mean (s.e.m).

Statistical differences were determined using the student's t–test or Kolmogorov–Smirnov test.

Immunohistochemical and Immunoblot Analyses

We blindly separated sister cultures into two groups for mock and curare treatment on day 6. After 24 hours, we rinsed cultures with PBS, fixed them with 4% formaldehyde in PBS for 7–10 min, blocked (1% BSA or 5% goat serum, 0.1% sapponin in PBS) for 30–60 min, then incubated cultures with primary antibody overnight at 4 °C. Antibodies against the following proteins were used at the indicated concentrations: Dα7 (1:200) [43], Shal (1:100) [46], syntaxin (1:200; Developmental Hybridoma Studies Bank (DHSB)), HA (1:200; Covance Research Products). After 4 washes (0.1% sapponin in PBS, 5 min each), we incubated cultures with fluorophore–conjugated secondary antibody (1:500; Jackson ImmunoResearch Laboratories) at room temperature for 1 hr, washed again, then mounted them in p–phenylenediamine in 90% glycerol. We imaged control and treated cultures with a 100X oil–immersion objective, under the same conditions (eg. exposure times) for comparison. For anti–HA or anti–Shal immunostaining, we determined average grey values from somas after substracting background grey values, using Photoshop CS2 software.

For immunoblot analyses, we used primary antibodies against the following proteins at the indicated concentrations, overnight at room temperature: Dα1 (pAb R14, 1:500)[47], Dα2 (mAb 4F6, 1:200)[48], Dα7 (1:200)[43], Dβ1 (mAb 3d2, 1:100)[49], Dβ2 (pAb 4596, 1:500)[50], Shal (1:100)[46], syntaxin (1:100; DHSB).

References

1. Turrigiano G. Too Many Cooks? Intrinsic and Synaptic Homeostatic Mechanisms in Cortical Circuit Refinement. Annu Rev Neurosci. 2011
2. Davis GW. Homeostatic control of neural activity: from phenomenology to molecular design. Annu Rev Neurosci. 2006; 29:307–23. [PubMed: 16776588]
3. Pozo K, Goda Y. Unraveling mechanisms of homeostatic synaptic plasticity. Neuron. 2010; 66:337–51. [PubMed: 20471348]
4. Desai NS, Rutherford LC, Turrigiano GG. Plasticity in the intrinsic excitability of cortical pyramidal neurons. Nat Neurosci. 1999; 2:515–20. [PubMed: 10448215]
5. Kuba H, Oichi Y, Ohmori H. Presynaptic activity regulates Na(+) channel distribution at the axon initial segment. Nature. 2010; 465:1075–8. [PubMed: 20543825]
6. Baines RA, Uhler JP, Thompson A, Sweeney ST, Bate M. Altered electrical properties in Drosophila neurons developing without synaptic transmission. J Neurosci. 2001; 21:1523–31. [PubMed: 11222642]
7. Nataraj K, Le Roux N, Nahmani M, Lefort S, Turrigiano G. Visual deprivation suppresses L5 pyramidal neuron excitability by preventing the induction of intrinsic plasticity. Neuron. 2010; 68:750–62. [PubMed: 21092863]
8. De Biasi M, Dani JA. Reward, Addiction, Withdrawal to Nicotine. Annu Rev Neurosci. 2011
9. Picciotto MR, Addy NA, Mineur YS, Brunzell DH. It is not “either/or”: activation and desensitization of nicotinic acetylcholine receptors both contribute to behaviors related to nicotine addiction and mood. Prog Neurobiol. 2008; 84:329–42. [PubMed: 18242816]
10. Fenster CP, Whitworth TL, Sheffield EB, Quick MW, Lester RA. Upregulation of surface alpha4beta2 nicotinic receptors is initiated by receptor desensitization after chronic exposure to nicotine. J Neurosci. 1999; 19:4804–14. [PubMed: 10366615]

11. Tsunoda S, Salkoff L. The major delayed rectifier in both Drosophila neurons and muscle is encoded by Shab. Journal of Neuroscience. 1995b; 15:5209–21. [PubMed: 7623146]
12. Tsunoda S, Salkoff L. Genetic analysis of Drosophila neurons: Shal, Shaw, and Shab encode most embryonic potassium currents. Journal of Neuroscience. 1995a; 15:1741–54. [PubMed: 7891132]
13. Lee D, O'Dowd DK. Fast excitatory synaptic transmission mediated by nicotinic acetylcholine receptors in Drosophila neurons. J Neurosci. 1999; 19:5311–21. [PubMed: 10377342]
14. Leung HT, Branton WD, Phillips HS, Jan L, Byerly L. Spider toxins selectively block calcium currents in Drosophila. Neuron. 1989; 3:767–72. [PubMed: 2642017]
15. Ping Y, et al. Shal/K(v)4 channels are required for maintaining excitability during repetitive firing and normal locomotion in Drosophila. PLoS One. 2011; 6:e16043. [PubMed: 21264215]
16. Su H, O'Dowd DK. Fast synaptic currents in Drosophila mushroom body Kenyon cells are mediated by alpha–bungarotoxin–sensitive nicotinic acetylcholine receptors and picrotoxin–sensitive GABA receptors. J Neurosci. 2003; 23:9246–53. [PubMed: 14534259]
17. Schmidt H, et al. The embryonic central nervous system lineages of Drosophila melanogaster. II. Neuroblast lineages derived from the dorsal part of the neuroectoderm. Dev Biol. 1997; 189:186–204. [PubMed: 9299113]
18. Gotti C, et al. Structural and functional diversity of native brain neuronal nicotinic receptors. Biochem Pharmacol. 2009; 78:703–11. [PubMed: 19481063]
19. Albuquerque EX, Pereira EF, Alkondon M, Rogers SW. Mammalian nicotinic acetylcholine receptors: from structure to function. Physiol Rev. 2009; 89:73–120. [PubMed: 19126755]
20. Aracava Y, Pereira EF, Maelicke A, Albuquerque EX. Memantine blocks alpha7* nicotinic acetylcholine receptors more potently than n–methyl–D–aspartate receptors in rat hippocampal neurons. J Pharmacol Exp Ther. 2005; 312:1195–205. [PubMed: 15522999]
21. Brickley SG, Revilla V, Cull–Candy SG, Wisden W, Farrant M. Adaptive regulation of neuronal excitability by a voltage–independent potassium conductance. Nature. 2001; 409:88–92. [PubMed: 11343119]
22. Pulver SR, Griffith LC. Spike integration and cellular memory in a rhythmic network from Na+/K+ pump current dynamics. Nat Neurosci. 2010; 13:53–9. [PubMed: 19966842]
23. Grauso M, Reenan RA, Culetto E, Sattelle DB. Novel putative nicotinic acetylcholine receptor subunit genes, Dalpha5, Dalpha6 and Dalpha7, in Drosophila melanogaster identify a new and highly conserved target of adenosine deaminase acting on RNA–mediated A–to–I pre–mRNA editing. Genetics. 2002; 160:1519–33. [PubMed: 11973307]
24. Griffith LC, et al. Inhibition of calcium/calmodulin–dependent protein kinase in Drosophila disrupts behavioral plasticity. Neuron. 1993; 10:501–9. [PubMed: 8384859]
25. Tripodi M, Evers JF, Mauss A, Bate M, Landgraf M. Structural homeostasis: compensatory adjustments of dendritic arbor geometry in response to variations of synaptic input. PLoS Biol. 2008; 6:e260. [PubMed: 18959482]
26. Kremer MC, et al. Structural long–term changes at mushroom body input synapses. Curr Biol. 2010; 20:1938–44. [PubMed: 20951043]
27. Bushey D, Tononi G, Cirelli C. Sleep and synaptic homeostasis: structural evidence in Drosophila. Science. 2011; 332:1576–81. [PubMed: 21700878]
28. Chou YH, et al. Diversity and wiring variability of olfactory local interneurons in the Drosophila antennal lobe. Nat Neurosci. 2010; 13:439–49. [PubMed: 20139975]
29. Lichtman JW, Colman H. Synapse elimination and indelible memory. Neuron. 2000; 25:269–78. [PubMed: 10719884]
30. Small DH. Network dysfunction in Alzheimer's disease: does synaptic scaling drive disease progression? Trends Mol Med. 2008; 14:103–8. [PubMed: 18262842]
31. Jerng HH, Pfaffinger PJ, Covarrubias M. Molecular physiology and modulation of somatodendritic A–type potassium channels. Mol Cell Neurosci. 2004; 27:343–69. [PubMed: 15555915]
32. Chen X, et al. Deletion of Kv4.2 gene eliminates dendritic A–type K+ current and enhances induction of long–term potentiation in hippocampal CA1 pyramidal neurons. J Neurosci. 2006; 26:12143–51. [PubMed: 17122039]

33. Kim J, Jung SC, Clemens AM, Petralia RS, Hoffman DA. Regulation of dendritic excitability by activity–dependent trafficking of the A–type K+ channel subunit Kv4.2 in hippocampal neurons. Neuron. 2007; 54:933–47. [PubMed: 17582333]
34. Cai X, et al. Unique roles of SK and Kv4.2 potassium channels in dendritic integration. Neuron. 2004; 44:351–64. [PubMed: 15473972]
35. Thiagarajan TC, Piedras–Renteria ES, Tsien RW. alpha– and betaCaMKII. Inverse regulation by neuronal activity and opposing effects on synaptic strength. Neuron. 2002; 36:1103–14. [PubMed: 12495625]
36. Groth RD, Lindskog M, Thiagarajan TC, Li L, Tsien RW. Beta Ca2+/CaM–dependent kinase type II triggers upregulation of GluA1 to coordinate adaptation to synaptic inactivity in hippocampal neurons. Proc Natl Acad Sci U S A. 2011; 108:828–33. [PubMed: 21187407]
37. Varga AW, et al. Calcium–calmodulin–dependent kinase II modulates Kv4.2 channel expression and upregulates neuronal A–type potassium currents. J Neurosci. 2004; 24:3643–54. [PubMed: 15071113]
38. Misonou H. Homeostatic regulation of neuronal excitability by K(+) channels in normal and diseased brains. Neuroscientist. 2011; 16:51–64. [PubMed: 20236949]
39. Magee JC, Cook EP. Somatic EPSP amplitude is independent of synapse location in hippocampal pyramidal neurons. Nat Neurosci. 2000; 3:895–903. [PubMed: 10966620]
40. Hoffman DA, Magee JC, Colbert CM, Johnston D. K+ channel regulation of signal propagation in dendrites of hippocampal pyramidal neurons. Nature. 1997; 387:869–75. [PubMed: 9202119]
41. Kazama H, Wilson RI. Homeostatic matching and nonlinear amplification at identified central synapses. Neuron. 2008; 58:401–13. [PubMed: 18466750]
42. Fujioka M, et al. Even–skipped, acting as a repressor, regulates axonal projections in Drosophila. Development. 2003; 130:5385–400. [PubMed: 13129849]
43. Fayyazuddin A, Zaheer MA, Hiesinger PR, Bellen HJ. The nicotinic acetylcholine receptor Dalpha7 is required for an escape behavior in Drosophila. PLoS Biol. 2006; 4:e63. [PubMed: 16494528]
44. Watson GB, et al. A spinosyn–sensitive Drosophila melanogaster nicotinic acetylcholine receptor identified through chemically induced target site resistance, resistance gene identification, and heterologous expression. Insect Biochem Mol Biol. 2010; 40:376–84. [PubMed: 19944756]
45. Hegde P, Gu GG, Chen D, Free SJ, Singh S. Mutational analysis of the Shab–encoded delayed rectifier K(+) channels in Drosophila. J Biol Chem. 1999; 274:22109–13. [PubMed: 10419540]
46. Diao F, Waro G, Tsunoda S. Fast inactivation of Shal (K(v)4) K+ channels is regulated by the novel interactor SKIP3 in Drosophila neurons. Mol Cell Neurosci. 2009; 42:33–44. [PubMed: 19463952]
47. Schulz R, et al. Neuronal nicotinic acetylcholine receptors from Drosophila: two different types of alpha subunits coassemble within the same receptor complex. J Neurochem. 2000; 74:2537–46. [PubMed: 10820216]
48. Jonas PE, Phannavong B, Schuster R, Schroder C, Gundelfinger ED. Expression of the ligand–binding nicotinic acetylcholine receptor subunit D alpha 2 in the Drosophila central nervous system. J Neurobiol. 1994; 25:1494–508. [PubMed: 7861114]
49. Chamaon K, Schulz R, Smalla KH, Seidel B, Gundelfinger ED. Neuronal nicotinic acetylcholine receptors of Drosophila melanogaster: the alpha–subunit dalpha3 and the beta–type subunit ARD co–assemble within the same receptor complex. FEBS Lett. 2000; 482:189–92. [PubMed: 11024458]
50. Chamaon K, Smalla KH, Thomas U, Gundelfinger ED. Nicotinic acetylcholine receptors of Drosophila: three subunits encoded by genomically linked genes can co–assemble into the same receptor complex. J Neurochem. 2002; 80:149–57. [PubMed: 11796753]

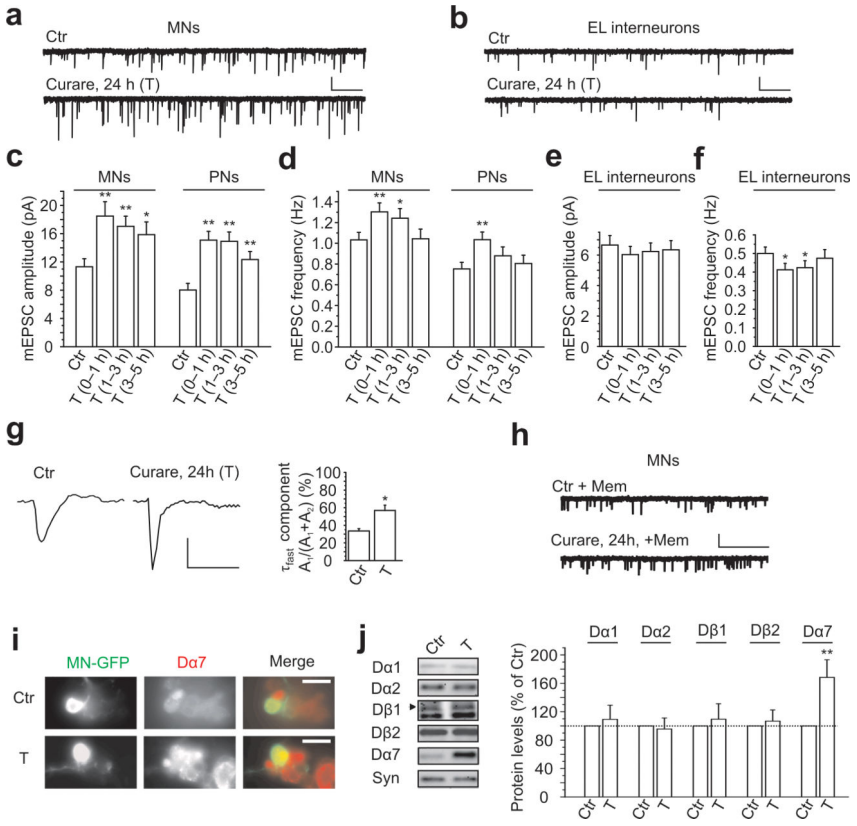

Figure 1. Synaptic Blockade Induces an Increase in Dα7 Receptors

(**a, b**) mEPSCs from MNs (A) and EL interneurons (B) in cultures mock (Ctr) and curare treated (T) for 24 hours. Scale bars represent 10 pA, 5 sec.

(**c, d**) mEPSC amplitude (**c**) and frequency (**d**) from Ctr and T cultures. n = 9–15.

(**e, f**) mEPSC amplitude (**e**) and frequency (**f**) from Ctr and T cultures from EL interneurons. n = 7–11.

(**g**) mEPSCs from Ctr and T cells (left). Deactivation of mEPSCs fit with a double exponential function; relative amplitude of τ(fast) component ($A_1/(A_1+A_2)$) (middle) are shown, n = 12 (Ctr) and 27 (T). Scale bars represent 10 pA, 5 ms. See also **Supplementary Figure 2**.

(**h**) mEPSCs recorded from MNs with memantine (Mem, 30 μM) from Ctr and T cultures (left). Mean (± s.e.m.) amplitudes showed no significant difference between Ctr and T cells. n = 12 (Ctr) and 10 (T). Scale bars represent 10 pA, 5 s.

(**i**) Ctr and T cultures immunostained for Dα7 (red); each cluster includes a single GFP–labeled MN. Scale bar represents 10 μm.

(**j**) Immunoblots (left), and quantification (right) of steady–state levels of Dα1, Dα2, Dα7, Dβ1 (arrow), and Dβ2 from Ctr and T brains. Protein levels normalized to Syntaxin (Syn) (n = 4). Error bars, s.e.m. **P* < 0.05 and ***P* < 0.01, Student's t test. See also **Supplementary Figure 3 and Table 1**. Full–length blots and gels are shown in **Supplementary Figure 9**.

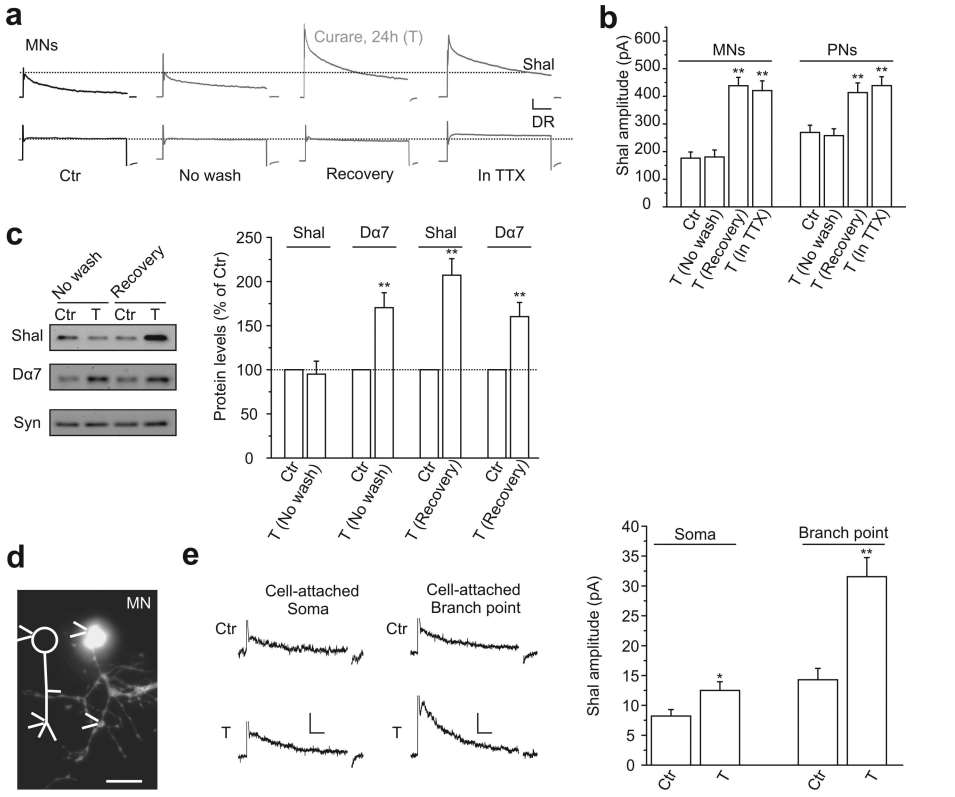

Figure 2. Inactivity Results in Increase in Shal Channels, Preferentially in Dendrites, Following Recovery of Synaptic Transmission

(**a**) Representative I_A (Shal) and delayed rectifier (DR) currents from MNs, separated by prepulse protocol, from Ctr (black) and 24–hr curare treated cultures (T, grey). Currents from treated cultures are shown with no antagonist washout (no wash; Protocol #2, see Methods), after antagonist washout and 30 min recovery (Recovery; Protocol #1, see Methods), and 30–min washout in TTX. Scale bars represent 100 pA, 25 ms.

(**b**) Quantitative analyses of currents represented in (A); shown for MNs and PNs. n = 10–17 for each condition.

(**c**) Representative imunoblots (left; 3 brains/lane) and quantitative analyses (right) for steady– state levels of Shal and Dα7 from Ctr, and T whole brain cultures without antagonist washout (T (No wash)) and with a 1–hr washout (T (Recovery)). n = 4.

(**d, e**) Cell–attached recordings from representative GFP–labeled MNs at the soma and branch point on dendrite (~30 μm from the soma), as indicated (**e**). Shown are representative Shal currents isolated by prepulse protocol, and quantitative analyses showing Shal amplitudes before and after curare treatment. Scale bars represent 10 μm (d), and 10 pA, 20 ms (e).

Error bars, s.e.m. **P* < 0.05 and ***P* < 0.01, Student's t test. See also **Supplemtentary Figure 2**. Full–length blots and gels are shown in **Supplementary Figure 9**.

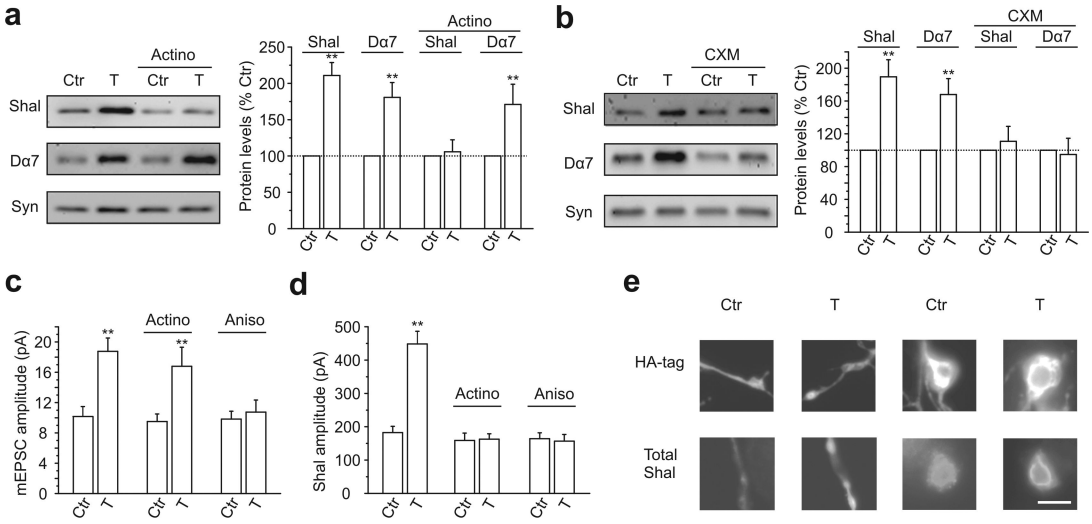

Figure 3. Dα7 and Shal Proteins Are Increased at the Translational and Transcriptional Level, Respectively

(**a, b**) Representative immunoblots (left), and quantitative analyses (right), for Dα7 and Shal from whole brain cultures following mock (Ctr) and curare treatment (30 μM, 24 hrs) (T; treatment Protocol #1, see Methods). Similar experiments are shown for brains incubated with Actinomycin D (Actino) (**a**), or cycloheximide (CXM) (**b**). n = 4. Syntaxin (Syn) was used as a loading control.

(**c, d**) Quatitative analyses of mEPSC (**c**) and I_A (Shal) (**d**) amplitudes from MNs following Ctr and T conditions; Actino or anisomycin (Aniso) were incubaded with cultures throughout treatment Protocol #1 (see Methods). n = 9–14 for each condition.

(**e**) Representative immunostaining for HA and Shal in MN dendrites (~50 μm for soma) and somas from transgenic line expressing HA–Shal. Note that after 24–hr curare treatment (T), there is an increase in total Shal signal, but no change in HA signal, in both dendrites and somas.

Error bars, s.e.m. $^{**}P < 0.01$, Student's t test. Full–length blots and gels are shown in **Supplementary Figure 10,** quantification of immunostaining is shown in **Supplementary Figure 4b**, and recorded Shal currents from Ctr and T HA–Shal expressing MNs are shown in **Supplementary Figure 4c.** Scale bar represents 10 μm.

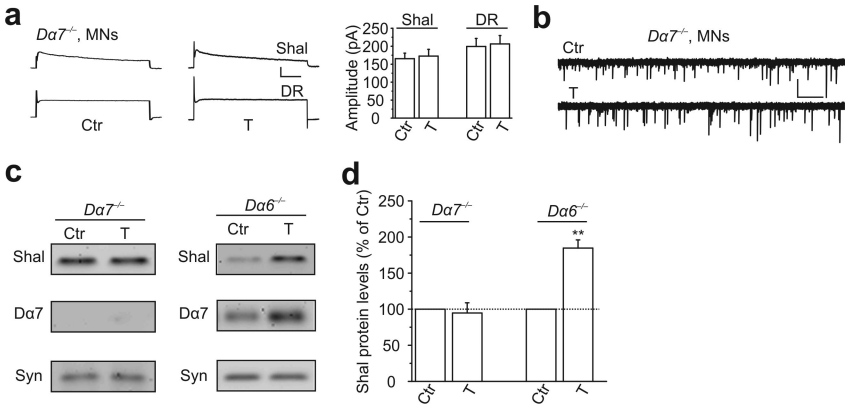

Figure 4. Dα7 Receptors are Essential for the Increased Expression of Shal Channels

(**a**) Representative I_A (Shal) and delayed rectifier (DR) currents isolated from mock (Ctr) and 24–hr curare treated (T) *Dα7*$^{P\Delta EY}$ (*Dα7*$^{-/-}$) mutant MNs (left); treatment Protocol #1 was used (see Methods). Quantitative analyses (right) shows no significant differences, for Shal or DR currents, between Ctr and curare treated cells (n = 15 for Ctr, 12 for T). Scale bars represent 100 pA, 25 ms.

(**b**) Representative mEPSCs from Ctr and T *Dα7*$^{P\Delta EY}$ (Dα7^{-}) mutant MNs (left). Scale bars represent 10 pA, 5 sec.

(**c–d**) Representative immunoblots (**c**), and quantitative analyses (**d**), of Shal and Dα7 protein levels in Ctr and T conditions from whole brains from *Dα7*$^{P\Delta EY}$ (*Dα7*$^{-/-}$) (left) and *Dα6*^{DAS2} (*Dα6*$^{-/-}$) (right) mutant flies. Syntaxin (Syn) was used as a loading control. Note Dα7 protein level was still increased in the curare treated brains from *Dα6*^{DAS2} mutant flies. n = 4 for each condition.

Error bars, s.e.m. $^{**}P < 0.01$, Student's t test. Full–length blots and gels are shown in **Supplementary Figure 10**.

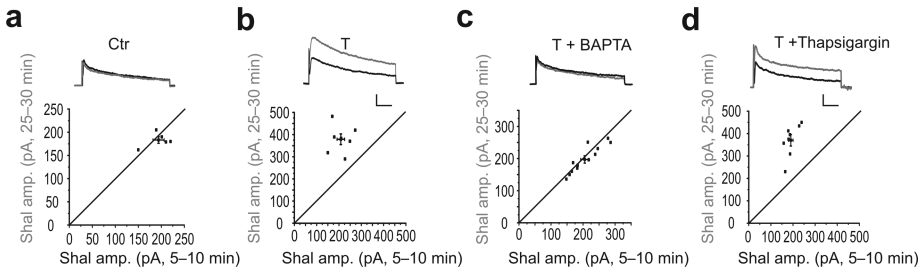

Figure 5. Ca^{2+} Influx Through Dα7 Receptors is Required for the Increase in Shal Channels

(**a, b**) Shal currents were recorded in MNs from cultures mock (**a**, Ctr), or curare treated (24 hrs treatment with 3 min washout of curare) (T) (**b**). Only the cells which were patched within 5–10 min after washout were used. Shal currents were continually monitored for the following 25–30 minutes. Representative Shal currents from Ctr and T conditions are shown: one trace from 5–10 min after washout (black), the other trace from the same cell at 25–30 min after washout (grey). Scatter plots of Shal amplitudes in individual cells at 5–10 min and 25–30 min are shown; means ± SEM are also indicated. n = 5–6 for each condition. Scale bars represent 100 pA, 25 ms.

(**c, d**) Representative traces and scatter plots from curare treated cultures; recording protocols similar to A and B. Recordings for (**c**) were performed in the conventional whole–cell mode with BAPTA included in the internal solution. Recordings for (**d**) were performed with thapsigargin preincubated in the external solution, and present throughout recordings. n = 8–12 for each condition. Scale bars represent 100 pA, 25 ms.

See also **Supplementary Figure 5**.

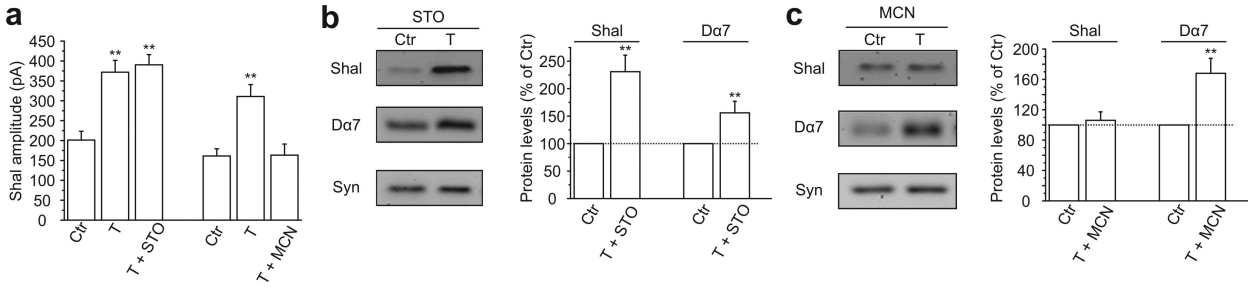

Figure 6. Activation of CaMKII, but not CaMKK, is Required for the Increase in Shal Channel Expression

(**a**) Quantitative analyses of Shal current amplitudes recorded from MNs in cultures mock (Ctr), or curare treated (30 μM, 24 hrs) (T); treatment Protocol #1 (see Methods) was used, with STO–609 (STO) or Myr–CaMKIINtide (MCN) present only during the recovery period and recording (n = 8–12 for each condition).

(**b, c**) Representative immunoblots (left) and quantitative analyses (right) of Shal and Dα7 protein levels in Ctr following T conditions, with STO or MCN present during washout only. Syntaxin (Syn) was used as a loading control. n = 4 for each condition.

Error bars, s.e.m. ***P* < 0.01, Student's t test. Full–length blots and gels are shown in **Supplementary Figure 10**.

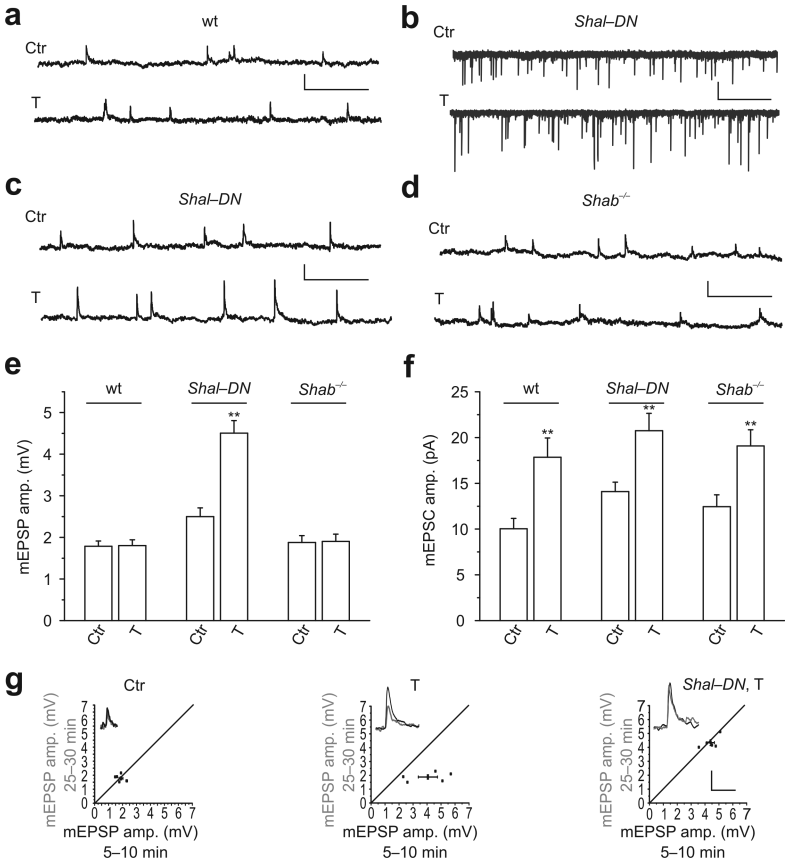

Figure 7. Increased Shal Channels Stabilize Synaptic Potentials

(**a, c, d**) Representative mEPSPs recorded from wild–type (wt) MNs (**a**), MNs expressing a dominant–negative Shal subunit (**c**, *Shal–DN*), and *Shab*^{3} MNs (**d**, *Shab*$^{-/-}$). MNs were either mock (Ctr), or curare treated (Protocol #1, see Methods) (T). Scale bars represent 2 mV, 1 s.

(**b**) mEPSCs from *Shal–DN* MNs in Ctr and T conditions. Scale bars represent 10 pA, 5 sec.

(**e**) mEPSP amplitudes for wt (n = 12–14), *Shal–DN* (n = 9–11), and *Shab*$^{-/-}$ (n = 9–11), Ctr and T MNs.

(**f**) mEPSC amplitudes from the same conditions as (**b**), from wt (n = 12), *Shal–DN* (n = 9–13), and *Shab*$^{-/-}$ (n = 12), Ctr and T MNs.

(**g**) mEPSPs from Ctr (left) and T (middle) wt MNs, or T MNs expressing *Shal–DN* (right). Cells were monitored after 3 min antagonist washout (Protocol #3, see Methods). Shown are mEPSPs recorded at 5–10 min after washout (black trace, inset), then again at 25–30 min (grey trace, inset). Scatter plots show mEPSP amplitudes from individual cells at 5–10 min and 25–30 min after washout; means are also indicated in plots. n = 5 for each condition. Scale bars represent 2 mV, 0.1 s.

Error bars, s.e.m. $^{**}P < 0.01$, Student's t test. See also **Supplementary Table 1**.